



ARTICLE

Genome-Wide Exploration of the Grape *GLR* Gene Family and Differential Responses of *VvGLR3.1* and *VvGLR3.2* to Low Temperature and Salt Stress

Honghui Sun^{1,2,#}, Ruichao Liu^{1,2,#}, Yueting Qi¹, Hongsheng Gao¹, Xueting Wang¹, Ning Jiang^{1,2}, Xiaotong Guo^{1,2}, Hongxia Zhang¹ and Chunyan Yu^{1,2,*}

¹The Engineering Research Institute of Agriculture and Forestry, Ludong University, Yantai, 264025, China

²College of Agriculture, Ludong University, Yantai, 264025, China

*Corresponding Author: Chunyan Yu. Email: yuchunyan@ldu.edu.cn

#These authors contributed equally to this work

Received: 06 January 2024 Accepted: 05 February 2024 Published: 28 March 2024

ABSTRACT

Grapes, one of the oldest tree species globally, are rich in vitamins. However, environmental conditions such as low temperature and soil salinization significantly affect grape yield and quality. The glutamate receptor (*GLR*) family, comprising highly conserved ligand-gated ion channels, regulates plant growth and development in response to stress. In this study, 11 members of the *VvGLR* gene family in grapes were identified using whole-genome sequence analysis. Bioinformatic methods were employed to analyze the basic physical and chemical properties, phylogenetic trees, conserved domains, motifs, expression patterns, and evolutionary relationships. Phylogenetic and collinear analyses revealed that the *VvGLRs* were divided into three subgroups, showing the high conservation of the grape *GLR* family. These members exhibited 2 glutamate receptor binding regions (GABAb and GluR) and 3–4 transmembrane regions (M1, M2, M3, and M4). Real-time quantitative PCR analysis demonstrated the sensitivity of all *VvGLRs* to low temperature and salt stress. Subsequent localization studies in *Nicotiana tabacum* verified that *VvGLR3.1* and *VvGLR3.2* proteins were located on the cell membrane and cell nucleus. Additionally, yeast transformation experiments confirmed the functionality of *VvGLR3.1* and *VvGLR3.2* in response to low temperature and salt stress. These findings highlight the significant role of the *GLR* family, a highly conserved group of ion channels, in enhancing grape stress resistance. This study offers new insights into the grape *GLR* gene family, providing fundamental knowledge for further functional analysis and breeding of stress-resistant grapevines.

KEYWORDS

Genome-wide identification; glutamate receptor (*GLR*) family; low temperature stress; salt stress; grape

1 Introduction

Glutamate receptor-like (*GLR*) protein, a crucial Ca^{2+} channel protein, facilitates Ca^{2+} influx from the extracellular space to the cytoplasm, inducing changes in the Ca^{2+} concentration [1]. There are two categories of glutamate receptors: metabotropic glutamate receptors (mGluRs) and ionotropic glutamate receptors (iGluRs). iGluRs are ligand-gated cation channels that respond to L-amino acids (such as glutamic acid



and glycine). They regulate excitatory nerve signal transmission and neuronal development in mammals [1] and are primarily expressed on the plasma membrane. The plant glutamate receptor (*GLR*) gene sequence is highly homologous to that of the animal *iGluR*. The earliest analysis of GLR in plants revealed 20 sequences homologous to iGluRs (AtGLRs) in *Arabidopsis thaliana* [2], categorized into three subfamilies: AtGLR1, AtGLR2, and AtGLR3 [3]. GLR proteins are highly conserved and feature two glutamate receptor binding regions (GABA_B and GluR) and 3-4 transmembrane regions (M1, M2, M3, and M4).

Glutamate receptors (*GLRs*) have been extensively studied in many plants, including *Arabidopsis*, rice, pear, apple, tomato, alfalfa, and sugarcane [4–10]. *GLRs* play an important role in regulating plant growth, influencing developmental phase such as seed germination [9], root development [10], apical meristem division and apoptosis [11], stomatal opening [9], pollen tube growth and morphogenesis [12,13], photosensitivity/phototropism in plants [5], light signal transduction [14], C/N balance regulation [15], water balance [16], calcium ion transport, and calcium-regulated stomatal movement [17]. Beyond growth and development, *GLRs* participate in biological and abiotic stress responses, such as alleviation of the toxic effects of aluminum ions [18]. For instance, *SIGLR3.3* and *SIGLR3.5* enhance drought tolerance in tomatoes [19], and *MtGLR* is involved in nitric oxide production in alfalfa during drought [7]. *OsGLR1* and *OsGLR2* improve drought tolerance in rice under drought stress conditions [20]. In *Arabidopsis*, *AtGLR1.1* controls development and water loss by regulating abscisic acid biosynthesis and signal transduction pathways [15]. Studies have also indicated that *AtGLR3.7* responds to salt stress [21], whereas *AtGLR1.2* and *AtGLR1.3* enhance low temperature tolerance in plants by activating the downstream *CBF/DREB1* pathway through jasmonic acid (JA) accumulation under low-temperature conditions [22–25].

Current research on *GLR* has been confined to the aforementioned species, however, the genome-wide exploration and expression patterns of GLRs in grapes remain unclear. This study utilized bioinformatic analysis methods to elucidate protein characteristics, offering valuable support for subsequent experiments and target selection. First, 11 grape *GLR* family genes were identified. To delve deeper into the structural characteristics, evolutionary relationships, and biological functions of the *GLR* genes in grapes, a comprehensive analysis was conducted. This analysis encompassed various bioinformatic features, such as structural domains, *cis*-acting promoter elements, protein structures, and protein-protein interactions. These findings suggest a pivotal role for *VvGLR* in conferring resistance to low temperature environments and salt stress.

2 Materials and Methods

2.1 Genomic Identification and Characterization of *VvGLRs* in Grapes

To identify the *GLR* gene family in grapes, the *Arabidopsis* *GLR* sequence from TAIR (<https://www.arabidopsis.org>) and grape *GLR* gene family information from the Ensemble database (<https://plants.ensembl.org/index.html>; release 51) served as a filter library. Using 20 *Arabidopsis* *GLRs* as a reference [2], local BLAST searches were conducted on grape protein sequences. Additionally, the login number and Hidden Markov model (HMM) file from pfam facilitated a hidden Markov model search for Lig_chan (PF00060) candidate proteins in two databases (Ensemble plants and Uniport) via HMMER 3.0. By comparing the outcomes of these screening methods and eliminating redundant protein sequences, grape *GLR* family members were ultimately identified [8]. The online platform ExPasy (www.expasy.org/) was applied to examine the molecular weight (MW), isoelectric point (PI), and total mean hydrophobicity (GRAVY) of the proteins. The online website (<http://www.csbio.sjtu.edu.cn/bioinf/Cell-PLoc-2>) was applied to predicate the subcellular localization of the *VvGLR* gene family [8].

2.2 Chromosome Distribution, Conserved Motifs, Gene Structure, and Three-Dimensional Domain Analysis

For gene chromosome positioning mapping, the GFF format file from the Ensemble plant database was obtained, and Graphics in TBtools were utilized. To investigate the conserved domain characteristics of the *GLR* gene family [26], the MEME database was applied to search conserved motifs.

2.3 Phylogenetic Analysis of GLRs from Different Plant Species

Sequences of *GLR* proteins from maize, rice, and Arabidopsis were submitted to ClustalW multiple sequence alignment using MUSCLE in MEGA 7.0. The NJ approach was utilized to generate a phylogenetic tree [2,10,27]. The p-distance module was applied for amino acid model selection, and 1000 bootstraps were performed. The major branches consistently displayed values between 95% and 100% [3]. Subsequently, the tree was refined using the online platform ITOL (<https://itol.embl.de/>) [10].

2.4 Synteny Relationship Analysis

To describe the collinearity of *GLRs* among diverse plant species, the genomic sequences of Arabidopsis and grape were obtained from Ensembl Plant database. The collinearity of genes between grape and Arabidopsis was determined by TBtools using Multiple Collinearity Scan Toolkit module [28].

2.5 Analysis of cis-Acting Elements of Grape GLR Family Promoter

For predicting the *cis*-acting elements of the grape *GLRs* promoter, the 2,000 bp sequence upstream of translation initiation codon of *VvGLRs* was downloaded from the Ensembl Plant database, and the PlantCARE database (<http://bioinformatics.psb.ugent.be/webtools/plantcare/html/>) was used [29]. Subsequently, the obtained information was visualized using TBtools software [8].

2.6 Prediction of Protein Structure and Interactions Based on the Network

A three-dimensional structural domain research of the *VvGLR* protein was conducted through SWISS-MODEL database (<https://swissmodel.expasy.org/>). To ensure model accuracy, the protein with the highest similarity to AtGLR was served as the template. The online website STRING (<https://cn.string-db.org>) was employed to predict genes that interact with the *VvGLR* family [21]. The OmicStudio platform (<https://www.omicstudio.cn/doc>) was employed to perform GO enrichment on genes that interacted with each other [8].

2.7 Gene Expression Analysis

To estimate gene expression, the TPM (per million transcripts) and FPKM (per million thousand base fragments) of *GLRs* in various grape parts were downloaded from the Grape eFP Browser (https://bar.utoronto.ca/efp_grape/cgi-bin/efpWeb.cgi). Subsequently TBtool was used to create heat maps for visualization [28].

2.8 Treatment of Plant Materials with Low Temperature and Salt Stress for Quantitative PCR Analysis

In this study, tissue-cultured 'Pinot Noir' grape plantlets were exposed to low temperatures of 4°C and -20°C in a growth chamber with 100 $\mu\text{mol m}^{-2} \mu\text{s}^{-1}$ light intensity and 16 h of light and 8 h of darkness. The standard culture temperature was 23°C, with consistent culture conditions. For the salt stress treatment, seven-week old tissue-culture seedlings cultivated on MS medium were transferred to Hoagland nutrient solution for 48 h to eliminate the potential effects of changing the culture conditions. Subsequently, seedlings were transferred to a solution containing either 0 or 100 mmol/L of NaCl. After 48 h of treatment, for total RNA extraction, the first and second completely grown leaves from the top of seedlings were gathered.

Total RNA from different treatments plants was extracted using the FastPure Plant Total RNA Isolation Kit (Polysaccharides & Polyphenolics-rich) (Vazyme, Nanjing, China), and the first-strand cDNA was synthesized through reverse transcription kit (Vazyme, Nanjing, China). RNA concentration and purity were estimated utilizing NanoDrop 2000 (Thermo Fisher Logical, Wilmington, DE, USA) and gel electrophoresis. To eliminate genomic DNA (gDNA) interference, RNA extraction was digested with a gDNA wiper (Vazyme, Nanjing, China) before first-strand cDNA synthesis. The SuperReal PreMix Plus (Tiangen, Beijing, China) was used for real-time quantitative PCR (qRT-PCR) analysis. Comparative CT method was used to calculate the relative expression levels [30]. *VvUBQ10* served as an endogenous reference gene for sample standardization, as described in a previous study [31]. To ensure experimental accuracy, each experiment was repeated three times. The gene-specific primers used for qRT-PCR are listed in Table S1.

2.9 Subcellular Localization of Grape GLR

To pinpoint the *VvGLR* gene, the full lengths of *VvGLR3.1* and *VvGLR3.2* were initially amplified, and a GFP subcellular localization vector was constructed. *Agrobacterium tumefaciens* strain GV3101 carrying 35 S:: GFP, 35 S:: GFP-*VvGLR3.1*, and 35 S:: GFP-*VvGLR3.2* was introduced into tobacco epidermal cells containing the red fluorescent proteins of H2B and a plasma membrane-located gene [4,32,33]. Tobacco epidermal cells were harvested after 2–3 d. A confocal laser microscope was used to observe and capture the fluorescence.

2.10 Vector Construction, Yeast Transformation and Stress Experiments

The protein expression vector pYES2 from *Saccharomyces cerevisiae* was constructed using ClonExpress II One Step Cloning Kit (Vazyme, Nanjing, China). Complete coding sequences of *VvGLR3.1* and *VvGLR3.2* were inserted into pYES2 and transformed into the host yeast strain INVSC1 for recombinant protein expression [34–38]. Subsequent salt stress experiments were conducted using SG-Ura (Coolaber, Beijing, China) media with NaCl concentrations of 0, 250, 500, and 750 mmol/L. The low-temperature experiment involved an initial culture at 4°C, 0°C, and –4°C for 48 h, followed by a switch to normal temperature for growth, and the growth status was observed [25].

2.11 Statistics Analysis

All data underwent variance analysis using IBM SPSS Statistics 20 [2]. Variance analysis was used to identify differences, and Student's *t*-test was applied to estimate the differences between mean values. Statistical significance was considered at 5% ($*p < 0.05$) or 1% ($**p < 0.01$) probability levels [2].

3 Results

3.1 Eleven *VvGLRs* Were Identified in the Grape Genome

In order to investigate the potential function of the GLR proteins in grapes, a total of 11 *GLR* coding genes were identified in the grape genome. Based on the naming rules of the *GLR* gene family [39] and considering their chromosomal positions, they were designated as *VvGLR 1.1*, *VvGLR2.1–VvGLR2.5*, and *VvGLR3.1–VvGLR3.5* (Table 1). Predicted full-length *VvGLR* consisted of 868 to 973 amino acid residues, with molecular weights ranging from 96.13 (*VvGLR 1.1*) to 108.81 kDa (*VvGLR 2.5*) and isoelectric points spanning from 5.59 (*VvGLR 2.1*) to 8.78 (*VvGLR 3.3*). Based on the positive total average hydrophilicity (GRAVY), all *VvGLRs* were predicted to be stable and hydrophobic proteins (Table 1). Subcellular localization prediction indicated that all *VvGLRs* were located in the plasma membrane.

Table 1: Information of *VvGLR* genes and their encoded proteins identified in the grape genome

Gene name	Gene ID	Protein size (aa)	pI	MW (kDa)	Localization prediction	Gravy
<i>VvGLR3.5</i>	Vitvi18g00071_t001	934	8.21	103038.24	Cell membrane	0.086
<i>VvGLR3.4</i>	Vitvi12g00517_t001	924	5.92	102779.43	Cell membrane	0.035
<i>VvGLR3.3</i>	Vitvi12g00516_t001	909	8.78	102420.32	Cell membrane	0.005
<i>VvGLR1.1</i>	Vitvi11g01251_t001	868	5.72	96127.07	Cell membrane	0.041
<i>VvGLR3.2</i>	Vitvi07g01890_t001	938	7.97	104091.21	Cell membrane	0.050
<i>VvGLR2.5</i>	Vitvi04g00725_t001	973	6.06	108807.86	Cell membrane	0.000
<i>VvGLR2.4</i>	Vitvi04g00716_t001	920	6.08	103088.75	Cell membrane	0.051
<i>VvGLR2.3</i>	Vitvi04g00715_t001	952	6.43	106358.25	Cell membrane	0.024
<i>VvGLR2.2</i>	Vitvi04g00712_t001	937	6.96	104431.17	Cell membrane	0.050
<i>VvGLR2.1</i>	Vitvi04g00696_t001	951	5.59	106230.78	Cell membrane	0.032
<i>VvGLR3.1</i>	Vitvi03g00246_t001	917	7.6	101529.41	Cell membrane	0.038

3.2 Structure of *VvGLR* Genes and Proteins Were Highly Conserved

Examination of the chromosomal distribution of the *VvGLR* family genes revealed an uneven and irregular spread across chromosomes 3, 4, 7, 11, 12, and 18 (Table S2). Specifically, *VvGLR3.1* was situated on chromosome 3, *VvGLR2.1*, *VvGLR2.2*, *VvGLR2.3*, *VvGLR2.4*, and *VvGLR2.5* were on chromosome 4, and *VvGLR3.2*, *VvGLR1.1*, and *VvGLR3.5* were found on chromosomes 7, 11, and 18, respectively. Chromosome 12 housed *VvGLR3.3* and *VvGLR3.4* (Fig. 1A). Their three-dimensional domains, protein motifs, and gene architectures were identified by further investigation. Among them, *VvGLR1.1*, *VvGLR2.1*, *VvGLR2.2*, *VvGLR2.3*, *VvGLR2.4*, and *VvGLR2.5* consisted of 5 exons, whereas the remaining *VvGLR3.1*, *VvGLR3.2*, *VvGLR3.3*, *VvGLR3.4*, and *VvGLR3.5*, contained 6 exons (Fig. 1B). Protein motif analysis highlighted the high conservation of GABAb and GluR domains in all *VvGLRs*, except for the Lig_chan domain on *VvGLR2.1*, *VvGLR2.2*, *VvGLR2.3*, and *VvGLR3.1*. MEME analysis divided the amino acid sequences of grape GLRs into 10 modules (Motif1–Motif10). With the exception of *VvGLR3.1*, *VvGLR3.2*, *VvGLR3.3*, and *VvGLR3.5*, which lacked motif1, each GLR contained nine conserved functional domains, motif2–motif10 (Fig. S1). In addition, all *VvGLRs* exhibited three to four transmembrane domains (M1–M4) (Figs. 1B and 1C). Based on the distribution of exons and introns, genes in both subfamilies of *VvGLR*, except for the third subfamily, contained 5 exons, whereas genes in the third subfamily contained 6 exons.

3.3 *VvGLRs* Contained Highly Conserved Protein Structures and the Protein-Protein Interactions Were Mostly Enriched in Ion-Binding Pathways

To understand the protein structure, a *VvGLR* protein structure model was constructed using AtGLR as a template. Analysis revealed that despite variations in length and structure among the 11 GLR proteins, they uniformly contained conserved structural domains, GABAb and GluR, which are typical structural features of *VvGLR* proteins (Fig. 2).

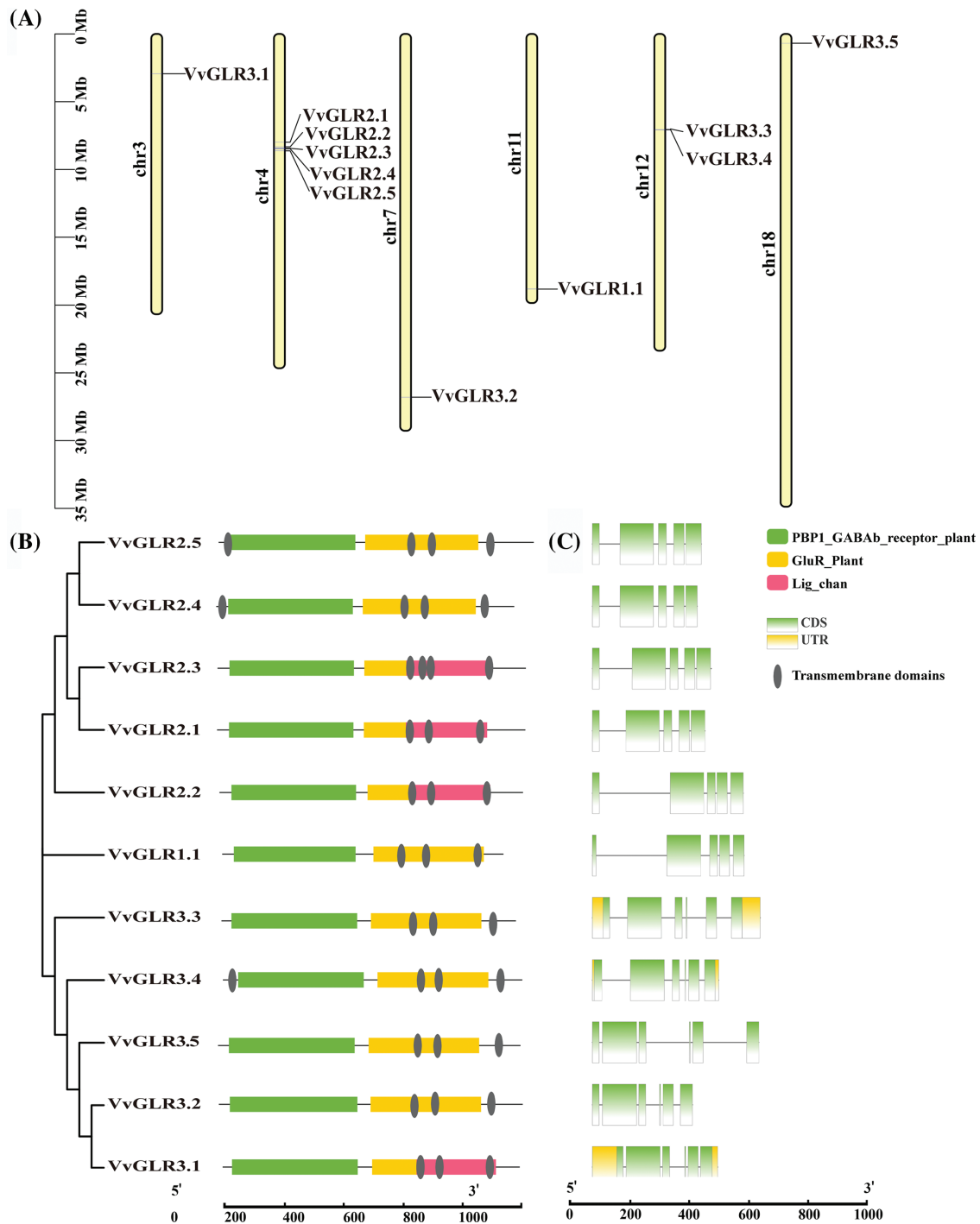


Figure 1: Analysis of chromosome distribution, phylogenetic relationships, conserved motifs and gene structure of VvGLRs. (A) VvGLR distribution on grape chromosomes. Chromosome sizes are indicated on the left using a scale. (B) Identification of conserved motifs in VvGLRs. Boxes with different colors represent various conserved motifs, and their relative position are displayed. A scale at the bottom is used to display sequence sizes (aa). (C) Exon-intron structures and phylogenetic tree of VvGLRs. Boxes with yellow, green, and black display un-translated regions (UTR), exons, and introns, respectively. The sequence sizes (bp) are shown on the bottom scale

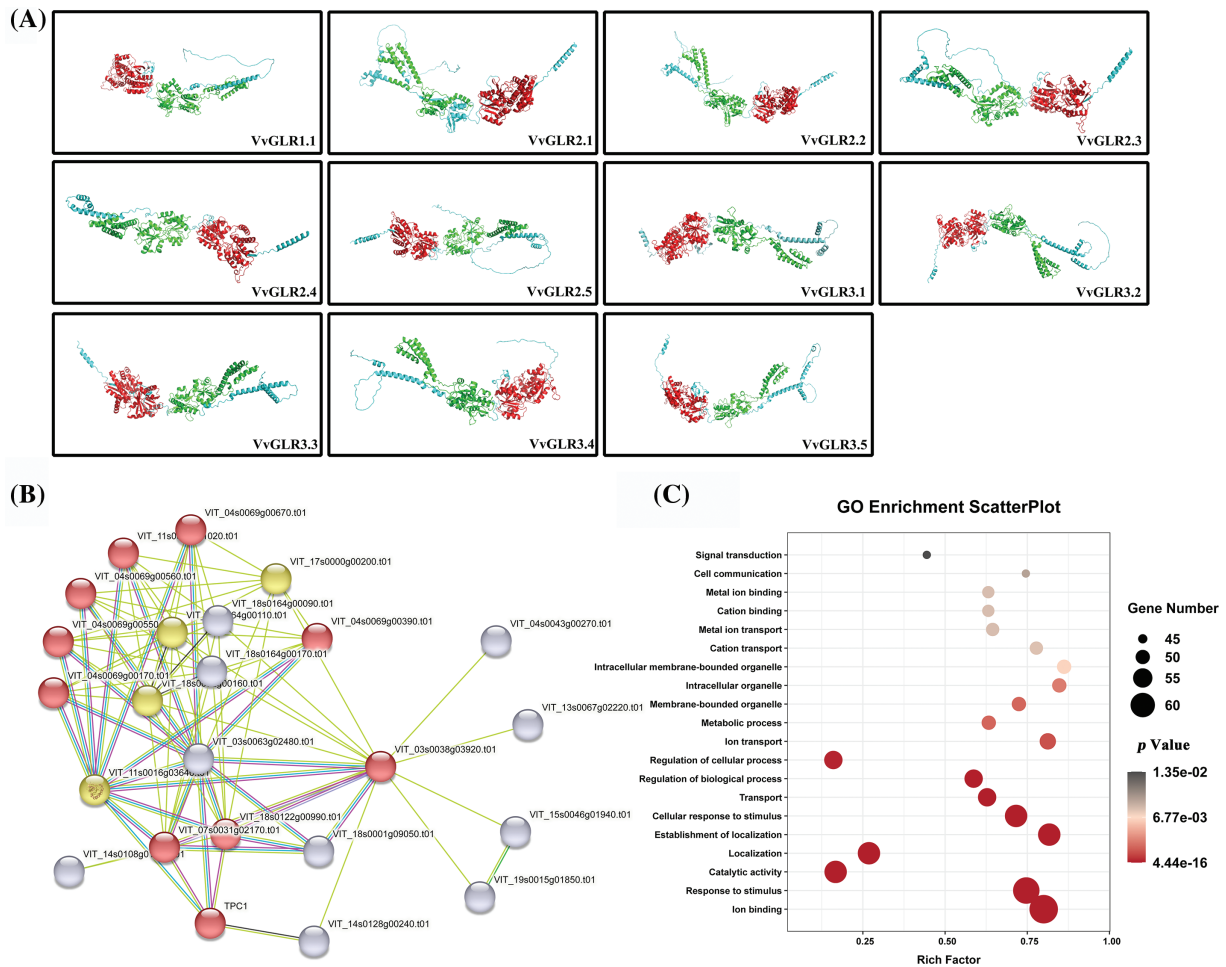


Figure 2: Three-dimensional structures of VvGLR proteins, GLR protein interaction network in grapes, and GO enrichment analysis. (A) Three-dimensional structures of VvGLR proteins with conserved GABA_B and GluR domains displayed by red and green, respectively. (B) Grape GLR proteins interaction network, where VvGLR family genes are marked with red circles. (C) Enrichment analysis of the proteins interacting with the VvGLR family. The color and size of the interactions indicate the reliability and frequency, respectively. A larger size signifies a higher interaction frequency, and a darker color signifies higher credibility

In the protein-protein interaction network, 14 proteins exhibited potential interactions with VvGLR proteins (Table S3). Functional enrichment analysis using the Gene Ontology database (<https://geneontology.org/>) demonstrated that these proteins were predominantly associated with biological processes, such as ion binding, response to stimuli, and catalytic activity. This result suggests that VvGLR proteins can respond to stimuli through ion binding.

3.4 VvGLRs Were Divided into Three Sub-Families

To elucidate the phylogenetic relationship between the GLR family proteins, a phylogenetic tree of the grape GLR gene family, along with 67 GLR protein sequences from two model plants (rice (20), Arabidopsis (20), and maize (16)), was constructed. Based on Arabidopsis and rice classifications, VvGLRs were categorized into three subfamilies, with 11 members distributed in Group I (1), Group II (5), and Group III (5). The phylogenetic tree illustrated that Groups I and II shared a common branch, and Group III (5).

I predated Group II, aligning with the notion that Group II in Arabidopsis might have evolved from a gene copy of Group I [40]. Compared with Group I, most of the *VvGLR* genes were situated in Groups II and III, suggesting potential versatility (Fig. 3, Table S4).

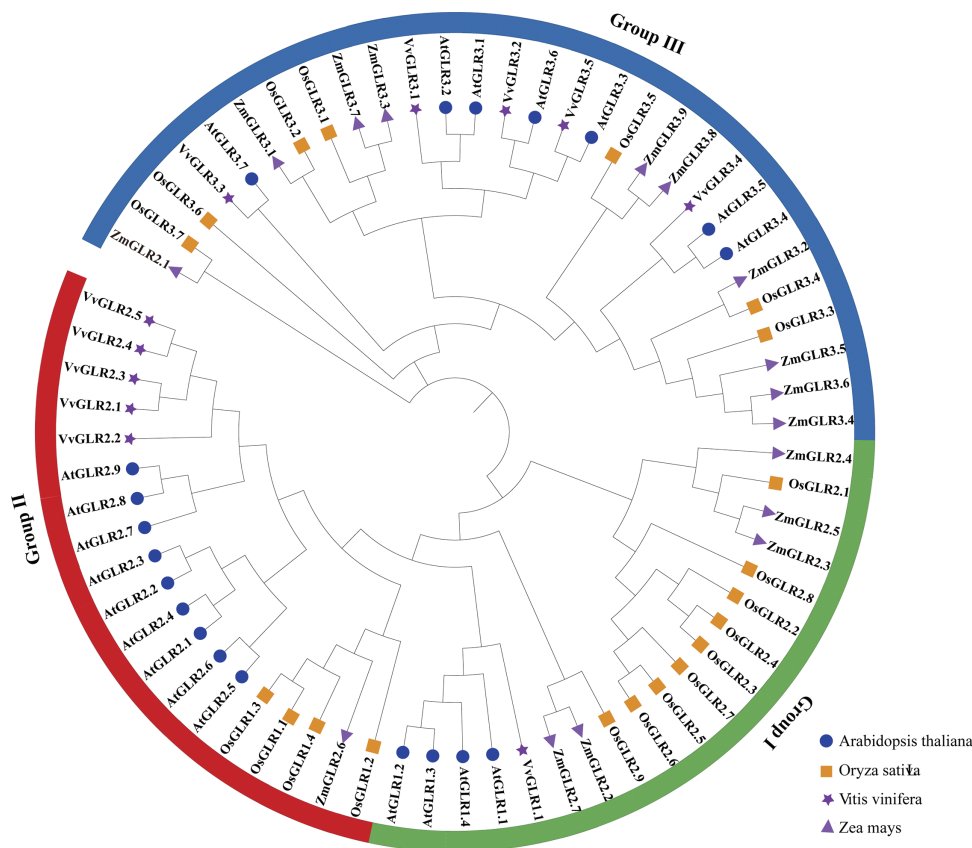


Figure 3: Phylogenetic analysis of GLR proteins from various species. A phylogenetic tree composed of 67 GLR proteins were divided into three groups (Groups I–III). Arabidopsis, rice, grape, and corn are represented by blue circles, orange squares, purple pentagons, and purple triangles, respectively. At, *Arabidopsis thaliana*; Os, *Oryza sativa*; Vv, *Vitis vinifera*; Zm, *Zea mays*

3.5 Analysis of Collinearity in Grape *VvGLR* Family

Gene replication, including whole-genome, tandem, and fragment replication, is a common occurrence in plant evolution [40,41]. However, no tandem repetition events have been observed in the grape *VvGLR* family. Collinearity analysis of Arabidopsis *AtGLR* and grape *VvGLR* was conducted, revealing a total of six pairs of orthologous genes (*VvGLR3.1* and *AtGLR3.1*, *VvGLR3.3* and *AtGLR3.4*, *VvGLR3.5* and *AtGLR3.3*, *VvGLR3.3* and *AtGLR3.5*, *VvGLR3.1* and *AtGLR3.2*, *VvGLR2.3* and *AtGLR2.4*) (Fig. 4). Consistent with the earlier phylogenetic tree branches, these were identified as homologous gene pairs, suggesting potentially shared or similar functions in plant growth and development, or reaction to stressful environments.

3.6 *VvGLRs* Contained Plant Hormones and *cis*-Acting Elements in Response to Stress

Analysis of the 2000 bp promoter sequence revealed the presence of regulatory elements involved in stress and plant hormone responses. Notably, the promoter region contained ABRE, TGACG-motif, MBS/MYB/MYC, and TCA-element, indicating their roles in plant regulation and hormonal responses.

Additionally, stress-related elements such as anti-inversion-related elements (TC-rich repeats), low-temperature response elements (CCGAAA), and environmental signal response elements (G-box) were identified (Fig. S2, Table S5). This suggests the potential involvement of the grape *VvGLR* family in the regulation of plant growth as well as in the response to various stress conditions.

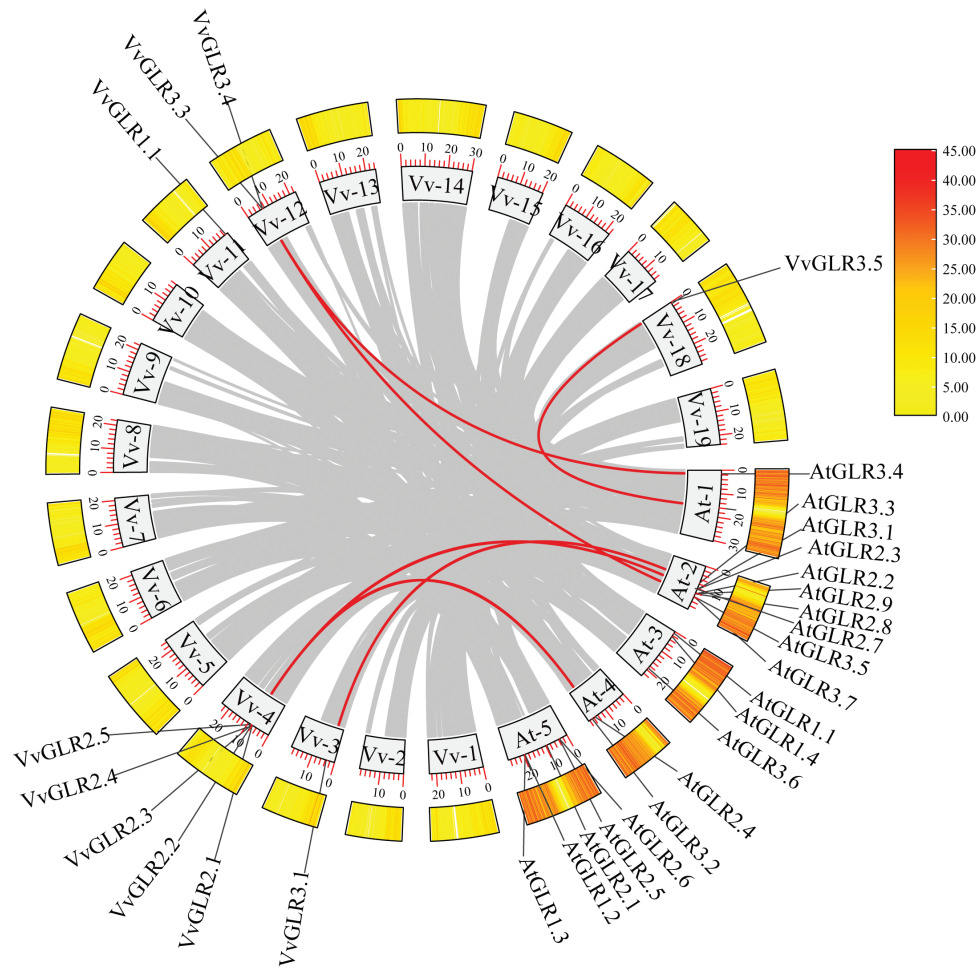


Figure 4: The synteny analysis of *VvGLRs*. Gray rectangles represent Arabidopsis and grapes chromosomes, with the numbers and length labeled on every chromosome. The distribution of *AtGLRs* and *VvGLRs* on each chromosome are displayed. Synteny relationships between *AtGLRs* and *VvGLRs* are indicated with red lines. Gray lines indicate the syntenic relationships of other genes. Vv and at represent *Vitis vinifera* and *Arabidopsis thaliana*, respectively

3.7 Analysis of Tissue-Specific Expression Patterns of Grape *VvGLR* Family Genes

Analysis of gene expression data from various grape tissues revealed varying degrees of expression of the *VvGLR* family genes across all grape parts (Fig. 5, Table S6), with relatively high expression levels in leaves. Notably, *VvGLR3.2*, *VvGLR3.3*, *VvGLR3.4*, and *VvGLR3.5* exhibited high expression in grape stems, vines, buds, shafts, and flesh. Transcriptome data indicated that during leaf development, *VvGLR3.1* was highly expressed in young leaves, whereas in the fruit setting stage, *VvGLR2.1*, *VvGLR1.1*, *VvGLR3.1*, *VvGLR2.2*, and *VvGLR3.4* displayed elevated expression. Additionally, during leaf aging, *VvGLR2.3*, *VvGLR2.4*, and *VvGLR2.5* showed high expression levels.

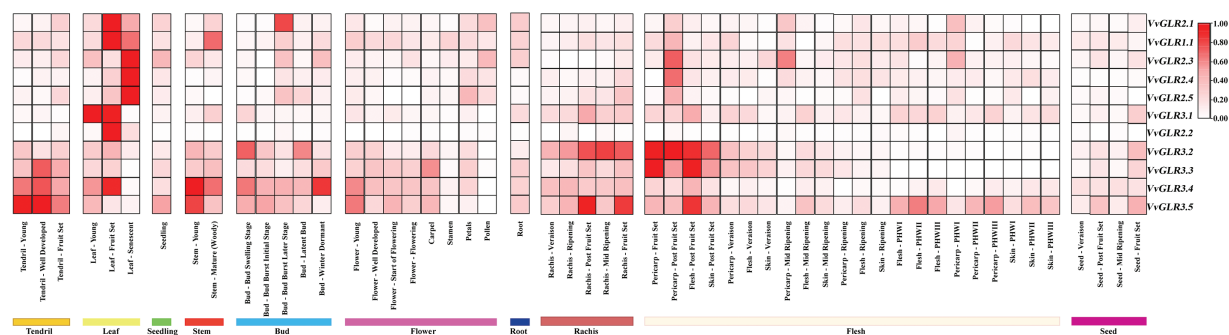


Figure 5: Expression heat map illustrating the developmental expression profiles of *VvGLRs* in various grape tissues, including tendrils, leaves, seeds, stems, buds, flowers, roots, rachises, and flesh. The estimated values expressed in transcripts per million (TPM) represent the expression levels of *VvGLRs*. The relative expression level of each gene is represented by the colored spectrum, which goes ranging from white to red

3.8 Differential Expression of *VvGLRs* under Cold and Salt Stress

To investigate the response and expression of the *VvGLR* gene to environmental stress, changes in *GLR* family gene expression were detected in the top two fully unfolded leaves of the grape seedlings. Real-time qRT-PCR analysis revealed the responsiveness of all *VvGLRs* to low temperature and salt stress (Fig. 6, Table S7). At 4°C, *VvGLR2.2*, *VvGLR2.3* and *VvGLR3.1* were upregulation, whereas *VvGLR1.1*, *VvGLR2.4*, *VvGLR2.5* and *VvGLR3.3* were downregulation. Notably, *VvGLR2.1*, *VvGLR3.2*, and *VvGLR3.5* exhibited rapid upregulation at 4 or 6 h, followed by a return to baseline expression after 48 h. *VvGLR2.3* and *VvGLR3.1* displayed an expression trend of a slight initial decrease followed by an overall increase. Under -20°C treatment simulating frost damage, *VvGLR2.3*, *VvGLR3.2*, *VvGLR3.3*, *VvGLR3.4* and *VvGLR3.5* showed overall upregulation, whereas *VvGLR1.1*, *VvGLR2.1*, *VvGLR2.2* and *VvGLR2.5* were downregulated. Among them, *VvGLR2.4* and *VvGLR3.1* were initially upregulated and then recovered to baseline after 48 h. Upon treatment with 100 mmol/L NaCl stress, *VvGLR2.4*, *VvGLR2.5*, *VvGLR3.1*, *VvGLR3.2*, *VvGLR3.3*, *VvGLR3.4* and *VvGLR3.5* exhibited overall upregulation, whereas *VvGLR1.1*, *VvGLR2.1*, *VvGLR2.2* and *VvGLR2.3* displayed a decreasing trend. Notably, *VvGLR3.1* and *VvGLR3.2* demonstrated increased sensitivity to low temperature and salt stress.

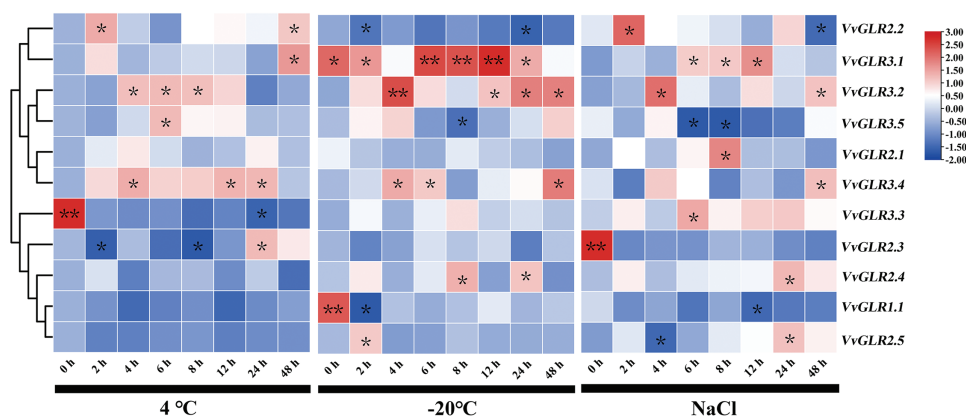


Figure 6: Heatmap analysis of the relative expression of *GLRs* under low temperatures (4°C and -20°C) and salt stresses. Seven-week old grape seedlings were exposed to 4°C and -20°C low temperatures and 100 mmol/L NaCl for 0, 2, 4, 6, 8, 12, 24, and 48 h. Values represent the means \pm standard deviation of three independent experiments (n = 3). A Student's *t*-test was judged at the probability of either 5% (* $p < 0.05$) or 1% (** $p < 0.01$)

3.9 Proteins of *VvGLR3.1* and *VvGLR3.2* Were Located on the Cell Membrane and Cell Nucleus

According to the PSORT website, the *VvGLR* family of proteins is predicted to be located on the cell membrane. A subsequent in-depth investigation into the subcellular localization of the *VvGLR* protein revealed that the GFP empty vector exhibited fluorescence in the nucleus, cell membrane, and cytoplasm of tobacco epidermal cells. Conversely, the fusion vector containing *VvGLR3.1* and *VvGLR3.2* proteins emitted fluorescence exclusively on the cell membrane and in the nucleus (Fig. 7). These results indicate their functional presence on both the cell membrane and the nucleus.

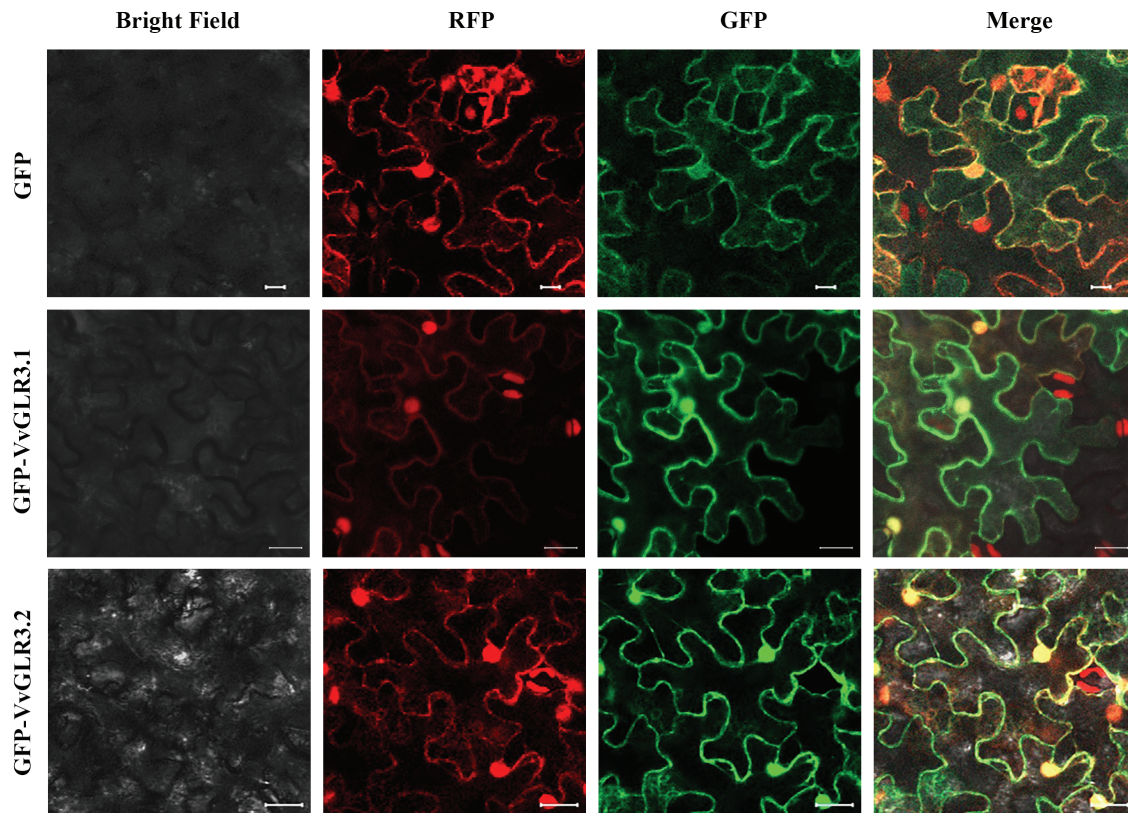


Figure 7: Subcellular localization of *VvGLR3.1* and *VvGLR3.2*. (*VvGLR3.1*-GFP and *VvGLR3.2*-GFP vectors along with plasma membrane localization protein were constructed and transiently transformed into tobacco epidermis). Scale bar = 20 μ m

3.10 Overexpression of *VvGLR3.1* and *VvGLR3.2* in Transgenic Yeast Increased Their Sensitivity to Low Temperature and Salt Stress

Because of the sensitivity of *VvGLR3.1* and *VvGLR3.2* to low temperature and salt stress, overexpression vectors for *VvGLR3.1* and *VvGLR3.2* were constructed to verify their function in response to abiotic stress. These vectors were then introduced into INVSC1 yeast strains. Yeast overexpressing *VvGLR3.1* and *VvGLR3.2* exhibited increased sensitivity to low temperature and various concentrations of salt stress compared to the wild type, manifesting significantly impaired growth in comparison to the control group (Fig. 8). This result substantiates the responsiveness of *VvGLR3.1* and *VvGLR3.2* to low temperature and salt stress.

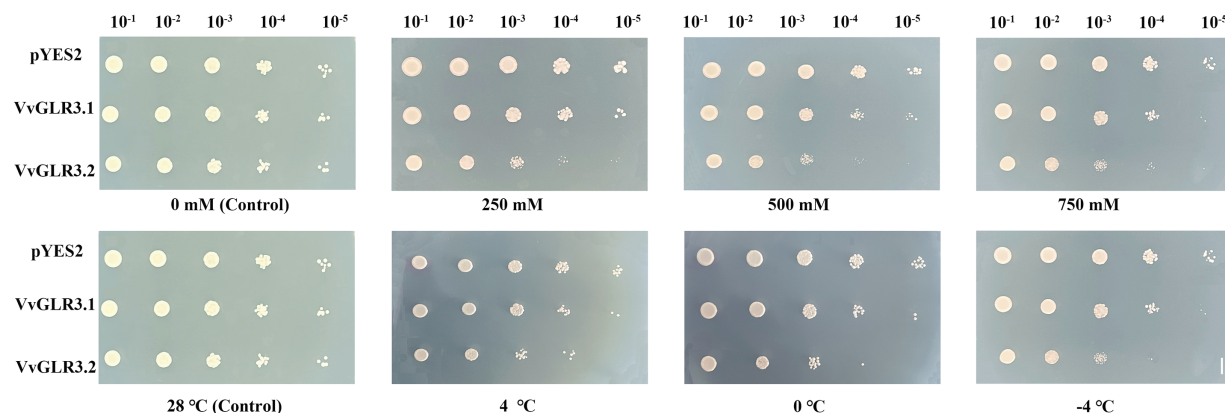


Figure 8: Growth of yeast overexpressing *VvGLR3.1* and *VvGLR3.2* under low temperature and salt stress conditions. Yeast cells harboring pYES2, pYES2-*VvGLR3.1*, or pYES2-*VvGLR3.2*, were grown in the SG-Ura synthetic dropout medium. Scale bar = 1 cm

4 Discussion

The Arabidopsis glutamate receptor gene *AtGLR*, discovered in 1998 [13] and highly homologous to mammalian *iGLuRs*, has paved the way for identifying *GLR* family genes in various plants, including rice, pear, tomato, maize, and alfalfa [4–10]. Despite this, research on their stress responses in grapes remains limited.

Studies indicate that *AtGLRs* in Arabidopsis and *GluRs* in animals share four transmembrane domains (M1, M2, M3, and M4) [3,15]. By leveraging the homology and structural similarity between *VvGLRs* in grapes and *AtGLRs* and *GluRs* in animals, we identified 11 *VvGLRs* that were distributed across six grape chromosomes. Consistent with other reports on *GLRs*, all *VvGLRs* exhibited GABA_B and *GluR* structural domains and 3–4 transmembrane domains, albeit with structural domain variations. Previous reports have indicated that the second transmembrane region M2 of *iGLuRs* cannot traverse the membrane [42]. This viewpoint was corroborated by transmembrane topology analysis of *AtGLRs* in Arabidopsis [43]. Therefore, some studies suggest that transmembrane M1 and M3, as well as non-transmembrane M2, correspond to the pore loop structure called the “hinge loop” in glutamate receptors [44], a common feature in ion channels [45,46]. Given the analogous gene structures and protein domains observed in *VvGLR2.1* and *VvGLR2.2*, as well as *VvGLR2.4* and *VvGLR2.5*, it is plausible that they have similar functions in grapes. Motif analysis revealed highly similar motifs across all grape *GLR* proteins, with no significant differences observed between members. This finding underscores the evolutionary stability of the grape *GLR* gene family. This study used phylogenetic analysis to examine the evolutionary history and relationships among species. The constructed phylogenetic tree categorized *VvGLRs* into three subgroups (Fig. 3). Notably, the majority of *VvGLRs* were concentrated in the second and third subgroups, comprising 90% of the total, aligning with similar patterns observed in other species [4–10].

Grape *GLR* exhibited 2 conserved domains and 3–4 transmembrane domains (Fig. 1B), mirroring the structural features of Arabidopsis and rice *GLRs* [2,12]. The motif distribution in the *VvGLR* varied among branches in the phylogenetic tree. Members of the same branch of the phylogenetic tree exhibited similar motif patterns. Phylogenetic and genetic structures indicated potential functional connections between them. This study highlights the correlation between the relative intron position/number and phylogenetic development. For example, *VvGLR2.4* and *VvGLR2.5* share a branch and similar gene structures. Phylogenetic relationships categorize *VvGLRs* into intron-poor and intron-rich groups

(Fig. 1C), with introns often associated with variable splicing in response to environmental changes, a conserved feature across species, such as rice and Arabidopsis [47,48]. This indicated that *VvGLR* is conserved across different species in terms of its gene structure.

Although the distribution of genes on chromosomes varies, their regulatory relationships depend on their function [49,50]. Therefore, this study analyzed the phylogenetic relationships and regulatory elements of *VvGLRs* (Fig. S2 and Table S3). Furthermore, this study delved into the relationship between the phylogeny of highly homologous gene pairs with significant differences and the regulatory elements in the promoter, such as *VvGLR2.1* and *VvGLR2.3*. Notably, this study examined the promoter region of *VvGLR* and identified numerous stress-responsive *cis*-acting elements. These elements have been identified in other species [2,12], many of which have been reported to respond to transcription factors and play regulatory roles [15,21].

Exploring the evolutionary and replication events of grape *GLR* genes sheds light on the intricate evolutionary processes of grapes. *VvGLR* was selectively located on chromosomes 3, 4, 7, 11, 12, and 18, suggesting evolutionary functions and intricate gene exchange. Gene expression patterns vary across vegetative and reproductive organs and developmental stages. Certain genes exhibit early-stage specificity, whereas others contribute to organ formation, providing pivotal insights into their biological functions [51–53]. This study meticulously analyzed the differential expression patterns of *VvGLR* across various grape tissues (Fig. 5), with notably elevated levels in the leaves and pulp, underscoring their roles in leaf development and pulp formation. Notably, *VvGLR3.2* and *VvGLR3.3* dominated in flowers, implicating their involvement in flowering regulation.

Previous studies have reported that GLRs are ubiquitously present in plant cells and participate in or mediate numerous physiological processes [3,47]. Subcellular localization prediction revealed their presence on the plasma membrane, aligning with their role as crucial ion channels that regulate Ca^{2+} flux [46]. Upon ligand activation, GLRs mediate Ca^{2+} influx across the plasma membrane to initiate downstream biological processes such as Ca^{2+} signal transduction during physiological and developmental events [54]. Consistent with GLRs reported in other species, *VvGLRs* were also predicted to be localized on the plasma membrane (Table 1). However, localization studies in *Nicotiana tabacum* confirmed that the proteins of *VvGLR3.1* and *VvGLR3.2* were located on both the cell membrane and cell nucleus. This finding, which is partially consistent with the predicted results, implies that *VvGLR3.1* and *VvGLR3.2* may share similar and distinct roles (Fig. 7). Maintaining cytoplasmic Ca^{2+} balance under normal and stressful growth conditions requires Ca^{2+} homeostasis, with various calcium transport proteins actively contributing, especially during non-biological stress and plant growth and development [55]. Previous studies have shown that *GLR* genes are found in various tissues, acting as receptor proteins pivotal in plant Ca^{2+} signal transduction and participating in diverse pathways throughout growth and development. Studies have indicated GLRs' responsiveness to stresses such as drought [20], salt stress [21,47,48,56], low-temperature stress [19], wilt disease [57], antifungal infection [5], and long-distance signal transduction triggered by both biological and non-biological stressors [26,58–60]. The carboxyl-terminal region of the glutamate receptor protein *GLR3.3* has been highlighted for its significant role in long-distance signal transduction induced by injury stimulation [60]. In this study, the *VvGLR* promoter region harbored multiple stress response elements, including those that respond to low temperatures, osmotic stress, and defense mechanisms. Real-time quantitative PCR analysis revealed the sensitivity of all *VvGLRs* to both low temperature and salt stress. Additionally, yeast transformation experiments proved the functionality of *VvGLR3.1* and *VvGLR3.2*, showing their responsiveness to low temperatures and salt stress. Given the extensive gene counts and intricate structures within the grape *GLR* gene family, further comprehensive research is essential to uncover additional gene functions. This study serves as a foundational step for the in-depth exploration of gene functions and regulatory mechanisms.

5 Conclusions

This study identified and thoroughly analyzed 11 grape *GLR* genes that were categorized into three subfamilies. Expression pattern analysis revealed predominantly constitutive expression among the *VvGLRs*, with all members exhibiting upregulation or downregulation in response to cold and salt stress. Overexpression of *VvGLR3.1* in *Saccharomyces cerevisiae* exhibited heightened sensitivity to both low temperatures and salt stress. Furthermore, *Saccharomyces cerevisiae* overexpressing *VvGLR3.2* displayed a phenotype similar to that observed with *VvGLR3.1*. These findings offer valuable insights into the functional aspects of the *VvGLRs* gene, shedding light on its potential role in enhancing grape tolerance to abiotic stress.

Acknowledgement: Thanks to all the reviewers who participated in the review, as well as MJEditor (www.MJEditor.com) for providing English editing services during the writing of this manuscript.

Funding Statement: This research was funded by the Natural Science Foundation of Shandong Province of China (ZR2022MC144).

Author Contributions: The authors confirm their contribution to the paper as follows: study conception and design: Honghui Sun, Ruichao Liu, Yueting Qi, and Hongsheng Gao; data collection: Ning Jiang, Xueting Wang; analysis and interpretation of results: Honghui Sun, Ruichao Liu, and Ning Jiang; draft manuscript preparation: Hongxia Zhang, Chunyan Yu, and Xiaotong Guo. All authors reviewed the results and approved the final version of the manuscript.

Availability of Data and Materials: Data are contained within the article and supplementary material.

Ethics Approval: None.

Conflicts of Interest: The authors declare that they have no conflicts of interest to report regarding the present study.

Supplementary Materials: The supplementary material is available online at <https://doi.org/10.32604/phyton.2024.049417>.

References

1. Zhu S, Gouaux E. Structure and symmetry inform gating principles of ionotropic glutamate receptors. *Neuropharmacology*. 2017;112:11–5.
2. Tapken D, Hollmann M. *Arabidopsis thaliana* glutamate receptor ion channel function demonstrated by ion pore transplantation. *J Mol Biol*. 2008;383(1):36–48.
3. Chiu JC, Brenner ED, DeSalle R, Nitabach MN, Holmes TC, Coruzzi GM. Phylogenetic and expression analysis of the glutamate-receptor-like gene family in *Arabidopsis thaliana*. *Mol Biol Evol*. 2002;19(7):1066–82.
4. Singh SK, Chien CT, Chang IF. The *Arabidopsis* glutamate receptor-like gene *GLR3.6* controls root development by repressing the Kip-related protein gene *KRP4*. *J Exp Bot*. 2016;67(6):1853–69.
5. Brenner ED, Martinez-Barboza N, Clark AP, Liang QS, Stevenson DW, Coruzzi GM. *Arabidopsis* mutants resistant to S(+)- β -methyl- α , β -diaminopropionic acid, a cycad-derived glutamate receptor agonist. *Plant Physiol*. 2000;124(4):1615–24.
6. Philippe F, Verdu I, Morère-Le Paven MC, Limami AM, Planchet E. Involvement of *Medicago truncatula* glutamate receptor-like channels in nitric oxide production under short-term water deficit stress. *Plant Physiol*. 2019;236:1–6.
7. Aouini A, Matsukura C, Ezura H, Asamizu E. Characterisation of 13 glutamate receptor-like genes encoded in the tomato genome by structure, phylogeny and expression profiles. *Gene*. 2012;493(1):36–43.

8. Zhang J, Cui T, Su Y, Zang S, Zhao Z, Zhang C, et al. Genome-wide identification, characterization, and expression analysis of glutamate receptor-like gene (*GLR*) family in sugarcane. *Plants*. 2022;11(18):2440.
9. Kong D, Ju C, Parihar A, Kim S, Cho D, Kwak JM. Arabidopsis glutamate receptor Homolog3.5 modulates cytosolic Ca²⁺ level to counteract effect of abscisic acid in seed germination. *Plant Physiol*. 2015;167(4):1630–42.
10. Li J, Zhu S, Song X, Shen Y, Chen H, Yu J, et al. A rice glutamate receptor-like gene is critical for the division and survival of individual cells in the root apical meristem. *Plant Cell*. 2006;18(2):340–9.
11. Michard E, Lima PT, Borges F, Silva AC, Portes MT, Carvalho JE, et al. Glutamate receptor-like genes form Ca²⁺ channels in pollen tubes and are regulated by pistil D-serine. *Science*. 2011;332(6028):434–7.
12. Wudick MM, Portes MT, Michard E, Rosas-Santiago P, Lizzio MA, Nunes CO, et al. CORNICHON sorting and regulation of *GLR* channels underlie pollen tube Ca²⁺ homeostasis. *Science*. 2018;360(6388):533–6.
13. Lam HM, Chiu J, Hsieh MH, Meisel L, Oliveira IC, Shin M, et al. *Glutamate-receptor* genes in plants. *Nature*. 1998;396(6707):125–6.
14. Hebda A, Liszka A, Lewandowska A, Lyczakowski JJ, Gabryś H, Krzeszowiec W. Upregulation of *GLRs* expression by light in Arabidopsis leaves. *BMC Plant Biol*. 2022;22(1):197.
15. Kang J, Turano FJ. The putative glutamate receptor 1.1 (*AtGLR1.1*) functions as a regulator of carbon and nitrogen metabolism in *Arabidopsis thaliana*. *Proc Natl Acad Sci USA*. 2003;100(11):6872–7.
16. Kang J. The putative glutamate receptor 1.1 (*AtGLR1.1*) in *Arabidopsis thaliana* regulates abscisic acid biosynthesis and signaling to control development and water loss. *Plant Cell Physiol*. 2004;45(10):1380–9.
17. Kim SA, Junemyoung K, Seul-Ki J, Myeong-Hyeon W, Honggil N. Overexpression of the *AtGluR2* gene encoding an Arabidopsis homolog of mammalian glutamate receptors impairs calcium utilization and sensitivity to ionic stress in transgenic plants. *Plant Cell Physiol*. 2001;42(1):74–84.
18. Sivaguru M, Pike S, Gassmann W, Baskin TIM. Aluminum rapidly depolymerizes cortical microtubules and depolarizes the plasma membrane: evidence that these responses are mediated by a glutamate receptor. *Plant Cell Physiol*. 2003;44(7):667–75.
19. Li H, Jiang X, Lv X, Ahammed GJ, Zhou Y. Tomato *GLR3.3* and *GLR3.5* mediate cold acclimation-induced chilling tolerance by regulating apoplastic H₂O₂ production and redox homeostasis. *Plant Cell Environ*. 2019;42(12):3326–39.
20. Lu G, Wang X, Liu J, Yu K, Gao Y, Liu H, et al. Application of T-DNA activation tagging to identify glutamate receptor-like genes that enhance drought tolerance in plants. *Plant Cell*. 2014;33(4):617–31.
21. Wang PH, Lee CE, Lin YS, Lee MH, Chen PY, Chang HC, et al. The glutamate receptor-like protein *GLR3.7* interacts with 14-3-3 ω and participates in salt stress response in *Arabidopsis thaliana*. *Front Plant Sci*. 2019;10:1169.
22. Achard P, Gong F, Cheminant S, Alioua M, Hedden P, Genschik P. The cold-inducible CBF1 factor-dependent signaling pathway modulates the accumulation of the growth-repressing DELLA proteins via its effect on gibberellin metabolism. *Plant Cell*. 2008;20:2117–29.
23. Shi Y, Tian S, Hou L, Huang X, Zhang X, Guo H, et al. Ethylene signaling negatively regulates freezing tolerance by repressing expression of *CBF* and type-A *ARR* genes in Arabidopsis. *Plant Cell*. 2012;24:2578–95.
24. Hu Y, Jiang L, Wang F, Yua D. Jasmonate regulates the inducer of CBF expression-C-repeat binding factor/DRE binding factor1 cascade and freezing tolerance in Arabidopsis. *Plant Cell*. 2013;25(8):2907–24.
25. Zheng Y, Luo L, Wei J, Chen Q, Yang Y, Hu X, et al. The glutamate receptors *AtGLR1.2* and *AtGLR1.3* increase cold tolerance by regulating jasmonate signaling in *Arabidopsis thaliana*. *Biochem Biophys Res Commun*. 2018;506(4):895–900.
26. Yu B, Liu N, Tang S, Qin T, Huang J. Roles of glutamate receptor-like channels (*GLRs*) in plant growth and response to environmental stimuli. *Plants*. 2022;11(24):3450.
27. Kumar S, Stecher G, Li M, Knyaz C, Tamura K. MEGA X: molecular evolutionary genetics analysis across computing platforms. *Mol Biol Evol*. 2018;35(6):1547–9.
28. Chen C, Chen H, Zhang Y, Thomas HR, Frank MH, He Y, et al. TBtools: an integrative toolkit developed for interactive analyses of big biological data. *Mol Plant Pathol*. 2020;13(8):1194–202.

29. Higo K, Ugawa Y, Iwamoto M, Korenaga T. Plant cis-acting regulatory DNA elements (PLACE) database: 1999. *Nucleic Acids Res.* 1999;27(1):297–300.
30. Schmittgen TD. Analyzing real-time PCR data by the comparative CT method. *Nat Protoc.* 2008;3(6):1101–8.
31. González-Agüero M, García-Rojas M, di Genova A, Correa J, Maass A, Orellana A, et al. Identification of two putative reference genes from grapevine suitable for gene expression analysis in berry and related tissues derived from RNA-Seq data. *BMC Genomics.* 2013;14:878.
32. Martin K, Kopperud K, Chakrabarty R, Banerjee R, Brooks R, Goodin MM. Transient expression in *Nicotiana benthamiana* fluorescent marker lines provides enhanced definition of protein localization, movement and interactions in planta. *Plant J.* 2009;59(1):150–62.
33. Nelson BK, Cai X, Nebenführ A. A multicolored set of in vivo organelle markers for co-localization studies in Arabidopsis and other plants. *Plant J.* 2007;51(6):1126–36.
34. Yang LM, Yang Q, Liu PG, Li S. Expression of the HSP24 gene from *Trichoderma harzianum* in *Saccharomyces cerevisiae*. *J Therm Biol.* 2008;33(1):1–6.
35. Min X, Lin X, Ndayambaza B, Wang Y, Liu W. Coordinated mechanisms of leaves and roots in response to drought stress underlying full-length transcriptome profiling in *Vicia sativa* L. *BMC Plant Biol.* 2020;20(1):165.
36. Huang R, Xiao D, Wang X, Zhan J, Wang A, He L. Genome-wide identification, evolutionary and expression analyses of LEA gene family in peanut (*Arachis hypogaea* L.). *BMC Plant Biol.* 2022;22(1):155.
37. Zhao H, Yao P, Zhao J, Wu H, Wang S, Chen Y, et al. A Novel R2R3-MYB transcription factor FtMYB22 negatively regulates salt and drought stress through ABA-dependent pathway. *Int J Mol Sci.* 2022;23(23):14549.
38. Obata T, Kitamoto HK, Nakamura A, Fukuda A, Tanaka Y. Rice shaker potassium channel OsKAT1 confers tolerance to salinity stress on yeast and rice cells. *Plant Physiol.* 2007;144(4):1978–85.
39. Lacombe B, Becker D, Hedrich R, DeSalle R, Hollmann M, Kwak JM, et al. The identity of plant glutamate receptors. *Science.* 2001;292(5521):1486–7.
40. Singh A, Kanwar P, Yadav AK, Mishra M, Jha SK, Baranwal V, et al. Genome-wide expressional and functional analysis of calcium transport elements during abiotic stress and development in rice. *FEBS J.* 2014;281(3):894–915.
41. Cheng L, Yuan HY, Ren R, Zhao SQ, Han YP, Zhou QY, et al. Genome-wide identification, classification, and expression analysis of amino acid transporter gene family in *Glycine Max*. *Front Plant Sci.* 2016;7:515.
42. Bennett JA, Dingledine R. Topology profile for a glutamate receptor: three transmembrane domains and a channel-lining reentrant membrane loop. *Neuron.* 1995;14(2):373–84.
43. Chiu J, Desalle R, Lam HM, Meisel L, Coruzzi G. Molecular evolution of glutamate receptors: a primitive signaling mechanism that existed before plants and animals diverged. *Mol Biol Evol.* 1999;16(6):826–38.
44. Mayer ML. Glutamate receptors at atomic resolution. *Nature.* 2006;440(7083):456–62.
45. MacKinnon R. Pore loops: an emerging theme in ion channel structure. *Neuron.* 1995;14(5):889–92.
46. Pantoja O. Recent advances in the physiology of ion channels in plants. *Annu Rev Plant Biol.* 2021;72:463–95.
47. Chen PY, Hsu CY, Lee CE, Chang IF. Arabidopsis glutamate receptor *GLR3.7* is involved in abscisic acid response. *Plant Signal Behav.* 2021;16(12):1997513.
48. Zhang H, Zhang Q, Zhai H, Li Y, Wang X, Liu Q, et al. Transcript profile analysis reveals important roles of jasmonic acid signalling pathway in the response of sweet potato to salt stress. *Sci Rep.* 2017;7:40819.
49. Filichkin SA, Hamilton M, Dharmawardhana PD, Singh SK, Sullivan C, Ben-Hur A, et al. Abiotic stresses modulate landscape of poplar transcriptome via alternative splicing, differential intron retention, and isoform ratio switching. *Front Plant Sci.* 2018;9:5.
50. Tran LS, Nakashima K, Sakuma Y, Simpson SD, Fujita Y, Maruyama K, et al. Isolation and functional analysis of Arabidopsis stress-inducible NAC transcription factors that bind to a drought-responsive cis-element in the early responsive to dehydration stress promoter. *Plant Cell.* 2004;16(9):2481–98.
51. Urao T, Yamaguchi-Shinozaki K, Urao S, Shinozaki K. An Arabidopsis *MYB* homolog is induced by dehydration stress and its gene product binds to the conserved *MYB* recognition sequence. *Plant Cell.* 1993;5(11):1529–39.

52. Han Y, Wan H, Cheng T, Wang J, Yang W, Pan H, et al. Comparative RNA-seq analysis of transcriptome dynamics during petal development in *Rosa chinensis*. *Sci Rep*. 2017;7:43382.
53. Monihan SM, Magness CA, Yadegari R, Smith SE, Schumaker KS. Arabidopsis CALCINEURIN B-LIKE10 functions independently of the SOS pathway during reproductive development in saline conditions. *Plant Physiol*. 2016;171(1):369–79.
54. Davenport R. Glutamate receptors in plants. *Ann Bot*. 2002;90(5):549–57.
55. Zhou L, Lan W, Chen B, Fang W, Luan S. A calcium sensor-regulated protein kinase, CALCINEURIN B-LIKE PROTEIN-INTERACTING PROTEIN KINASE19, is required for pollen tube growth and polarity. *Plant Physiol*. 2015;167(4):1351–60.
56. Cheng Y, Zhang X, Sun T, Tian Q, Zhang WH. Glutamate receptor Homolog34 is involved in regulation of seed germination under salt stress in Arabidopsis. *Plant Cell Physiol*. 2018;59(5):978–88.
57. Liu S, Zhang X, Xiao S, Ma J, Shi W, Qin T, et al. A single-nucleotide mutation in a GLUTAMATE RECEPTOR-LIKE gene confers resistance to fusarium wilt in *Gossypium hirsutum*. *Adv Sci*. 2021;8(7):2002723.
58. Shao Q, Gao Q, Lhamo D, Zhang H, Luan S. Two glutamate- and pH-regulated Ca²⁺ channels are required for systemic wound signaling in Arabidopsis. *Sci Signal*. 2020;13(640):eaba1453.
59. Mousavi SA, Chauvin A, Pascaud F, Kellenberger S, Farmer EE. *GLUTAMATE RECEPTOR-LIKE* genes mediate leaf-to-leaf wound signalling. *Nature*. 2013;500(7463):422–6.
60. Wu Q, Stolz S, Kumari A, Farmer EE. The carboxy-terminal tail of *GLR3.3* is essential for wound-response electrical signaling. *New Phytol*. 2022;236(6):2189–201.